



Low-density polyethylene films incorporated with silver nanoparticles to promote antimicrobial efficiency in food packaging

Sabrina da Costa Brito^{1,2} , Joana D Bresolin², Kátia Sivieri¹ and Marcos D Ferreira^{1,2} 

Abstract

Technological innovations in packaging are intended to prevent microbiological contaminations for ensuring food safety and preservation. In this context, researchers have investigated the antimicrobial effect of low-density polyethylene films incorporated with the following concentrations of silver nanoparticles: 1.50, 3.75, 7.50, 15.00, 30.00, 60.00, and 75.00 µg/ml. The films were characterized using field emission gun scanning electron microscopy, Fourier transform infrared spectroscopy, X-ray diffraction, thermogravimetry, and differential scanning calorimetry. From the results of these techniques, it could be concluded that the silver nanoparticles incorporated in the low-density polyethylene films did not influence their physical, chemical, and thermal properties. The direct contact assays, shake-flask assays, and bacterial images obtained using scanning electron microscopy were used to analyze the antimicrobial activity of the films. In the microbial analyses, it was verified that the nanostructured films exhibited antimicrobial properties against all the microorganisms studied, although more notably for fungi and Gram-negative bacteria than the Gram-positive bacteria. Moreover, it was discovered that the packages, in which silver nanoparticles were incorporated, inhibited the growth and reproduction of bacterial cells during the early stages. These results suggest that the extruded low-density polyethylene films incorporated with silver nanoparticles may be an essential tool for improving food quality and safety.

Keywords

Polyethylene, silver nanoparticles, antimicrobial, food packaging

Date received: 24 March 2019; accepted: 6 November 2019

INTRODUCTION

Packaging materials are mainly intended to protect food against spoilage processes due to chemical, physical, or biological contaminations and oxidation from storage until final consumption to maintain the characteristics of the food for a more extended post-processing period (Gava et al., 2008; Piringir and Baner, 2000; Wróblewska-Krepsztul et al., 2018; Youssef and El-Sayed, 2018).

In this context, technological innovations with respect to advanced and multifunctional packaging are intended to optimize the prevention of food contamination, particularly those arising from microorganisms, leading to enhanced food safety and preservation (Akter et al., 2018; Brody et al., 2008; Carbone et al.,

¹School of Pharmaceutical Sciences, São Paulo State University (UNESP), Araraquara, Brazil

²Brazilian Agricultural Research Corporation (EMBRAPA), Embrapa Instrumentation, São Carlos, Brazil

Corresponding author:

Sabrina da Costa Brito, School of Pharmaceutical Sciences, São Paulo State University (UNESP), Rodovia Araraquara Jaú, Km 01—s/n—Campos Ville, Araraquara 14801-902, Brazil.
Email: scbrito@yahoo.com.br

2016; Marsh and Bugusu, 2007; Mihindukulasuriya and Lim, 2014; Wróblewska-Krepsztul et al., 2018).

Nanotechnology applied to food packaging has been searching for alternatives that had been previously considered to be obstacles, as nanotechnology can be used to prepare antimicrobial agents for increasing the shelf life of foods during storage and distribution (Chaudhry et al., 2008; Youssef and El-Sayed, 2018). As a consequence, a new active and intelligent packaging generation, which comprises metal nanoparticle-containing nanostructured packaging, has emerged to reduce the microbial load of food products (Greiner, 2009).

The metal nanoparticles' feature improved antimicrobial efficiency due to their increased surface-area-to-volume ratio (Damm et al., 2005). Among these, the silver nanoparticles (AgNPs) demonstrate the most intense antimicrobial activity (Akter et al., 2018; Kim et al., 2007; Ruparelia et al., 2008; Siddiqi et al., 2018; Sonidi and Salopek-Sonidi, 2004). They are also one of the substances that are more frequently combined with polymer-based materials (Becaro et al., 2015; Dehnavi et al., 2012; Jokar et al., 2012) owing to their unique properties, such as high thermal stability and chemical compatibility with polymer matrices of low-density polyethylene (LDPE), which are not observed in other antimicrobial agents (Carbone et al., 2016; Chen and Schluesener, 2008; Duncan, 2011; Jokar et al., 2012).

LDPE is a polymer that is typically used in various economic segments within the food industry because it is flexible, transparent, processible, and thermally stable (Del Nobile et al., 2009; Marsh and Bugusu, 2007). Becaro et al. (2015) observed a stronger antimicrobial activity of silver nanocomposite LDPE films against *Staphylococcus aureus* and *Escherichia coli* by conducting the Japanese Industrial Standard test (JIS), and Jokar et al. (2012) also noticed a significant antimicrobial activity of AgNPs + LDPE against *S. aureus*, *E. coli*, and *Candida albicans* through a disk diffusion test. Using fresh-cut carrots packaged with silver nanoparticles incorporated in LDPE, Becaro et al. (2016) verified the antibacterial capability in lower concentrations of AgNPs against mesophilic aerobic and coliforms. These films also maintained the ascorbic acid content of fresh-cut carrots with minimal weight loss. Moreover, Emamifar et al. (2011) observed a significant decrease in fungi and total bacteria populations along with a reduced browning index and improved ascorbic acid retention in orange juice that is packaged in silver nanocomposite films.

In this work, LDPE films with varying concentrations of silver nanoparticles were prepared. Field emission gun scanning electron microscopy (FEG-SEM), Fourier transform infrared (FTIR) spectroscopy, X-ray diffraction (XRD), and thermal analyses were

employed to characterize these films. The antimicrobial action of these films was evaluated by direct contact assay, shake-flask assay, and bacterial images obtained from scanning electron microscopy (SEM), aiming to generate widespread applications of this material in food packaging.

MATERIALS AND METHODS

Materials

LDPE-based masterbatch, which comprises AgNPs in concentrations of 1.50, 3.75, 7.50, 15.00, 30.00, 60.00, and 75.00 µg/ml, was dispersed within a silica (SiO₂) matrix in the LDPE film (Table 1). The AgNP-free LDPE film was used as the control film. The masterbatches were obtained from a nanotechnology company, and the films were produced in a plastic packaging factory. Both companies are based in São Paulo, Brazil.

Film preparation

The masterbatches and pure LDPE pellets (LDPE 583) were mixed in plastic bags for 3 min in distinct concentrations (Table 2) and extruded in films by a plastic benchtop single screw extruder (AX Plastic). These mixtures were added to the extruder that comprises three different heating zones at 160 °C (zone 1), 145 °C (zone 2), and 130 °C (zone 3) and operates at a screw speed of 35 r/min (Becaro et al., 2015).

Film characterization

FEG-SEM. The morphological characteristics of the AgNP-containing films were investigated by detecting backscattered electrons through FEG-SEM using a JSM-6701F/JEOL microscope. Films were sectioned and fixed in stubs for obtaining the surface images. For cross-sectional images, films were cryo-fractured

Table 1. Percentage per masterbatch (%) for varied AgNP and SiO₂ content concentrations (µg/ml)

Masterbatch (%)	AgNP concentration (µg/ml)	SiO ₂ concentration (µg/ml)
2	1.50	298.50
5	3.75	746.25
10	7.50	1492.50
20	15.00	2985.00
40	30.00	5970.00
80	60.00	11,940.00
100	75.00	14,925.00

Table 2. AgNP concentration in LDPE film ($\mu\text{g/ml}$) for each percentage compositional ratio between masterbatch and LDPE (%)

AgNP concentration ($\mu\text{g/ml}$)	Masterbatch: LDPE (%)
1.50	2:99.99970
3.75	5:99.99925
7.50	10:99.99850
15.00	20:99.99700
30.00	40:99.99400
60.00	80:99.98800
75.00	100:99.98500

LDPE: low-density polyethylene.

in liquid nitrogen and fixed similarly. The samples were then carbon-coated on an evaporator and imaged. Moreover, the Ag + SiO_2 powder additive was also analyzed.

FTIR spectroscopy. The FTIR spectrometer Perkin Elmer, model Spectrum 1000, was used to detect vibrational frequencies. Control and nanostructured specimens were analyzed using 64 scans at wavenumbers ranging from 4000 to 400 cm^{-1} with a resolution of 4 cm^{-1} . Film specimens without prior preparation were attached to the support, and the FTIR spectra were recorded using the transmittance method.

XRD. A Shimadzu diffractometer model 6000 was used to determine the atomic structures of the films and Ag + SiO_2 powder additive, in which control and nanostructured samples without prior treatments were attached using a standard glass holder. Once in the X-ray generation chamber, the samples were analyzed at a 30 kV acceleration voltage, 30 mA current, 0.5° per min^{-1} , and 2θ ranging between 4° and 90° .

Thermal analyses. Thermogravimetry (TG) was used to investigate the thermal stability of the film. A thermogravimetric analyzer TGA Q 500 (TA Instruments) was used to analyze the samples (10 mg) at a heating rate of 10°C/min from 10 to 800°C . Nitrogen and synthetic air flows were provided at 40 and 60 ml/min , respectively.

To identify the endothermic and exothermic events in the 10 mg film samples upon heating, a DSC Q 100 (TA Instruments) was used for differential scanning calorimetry (DSC) runs. Tests were conducted at temperatures ranging from 10 to 200°C , using a heating rate at 10°C/min in a nitrogen atmosphere flowing at 60 ml/min .

Microbiological evaluations

Direct contact assays, shake-flask assays, and bacterial images were obtained by performing SEM on the Gram-positive bacteria *S. aureus* (INCQS 15 ATCC 25923) and *Enterococcus faecalis* (INCQS 234 ATCC 29212), Gram-negative bacteria *E. coli* (INCQS 33 ATCC 25922) and *Salmonella enterica* subsp. *enterica* serovar Typhimurium (INCQS 84 ATCC 13311), and apple-isolated *Penicillium expansum* (PEN001). The AgNP-free LDPE films were used as the control in all these tests. The antibiotic streptomycin sulfate (Sigma-Aldrich) ($3000\text{ }\mu\text{g/ml}$) was used as the positive control for *S. aureus*, *S. Typhimurium*, and *Escherichia*, whereas levofloxacin (Novartis) ($0.25\text{ }\mu\text{g/ml}$) and the antifungal itraconazole (EMS) ($16\text{ }\mu\text{g/ml}$) were used as positive controls for *E. faecalis* and *P. expansum*, respectively.

Direct contact assay. Bacterial colonies were inoculated in 10 ml of tryptic soy broth (TSB) (Kasvi) and incubated at 37°C for 24 h. Then, each microorganism was centrifuged (Hettich Zentrifugen Rotina-390) for 5 min at 10°C and 2000 r/min . The supernatant was discarded, and the cells were re-suspended in the saline solution (0.9%). Each microorganism inoculum was adjusted to provide a final concentration of $1.14 \times 10^5\text{ log CFU/ml}$ for *S. aureus*, $0.58 \times 10^5\text{ log CFU/ml}$ for *E. faecalis*, $1.12 \times 10^5\text{ log CFU/ml}$ for *E. coli*, and 1.03×10^5 for *S. Typhimurium* in log CFU/ml through absorbance readings at 600 nm on an ultraviolet-visible (UV-VIS) spectrometer (Shimadzu UV 1650) (Pagno et al., 2015).

The control and AgNP-containing films were shaped into $4\text{ cm} \times 4\text{ cm}$ (16 cm^2) squares, disinfected by immersing in 70% ethyl alcohol for 15 min, and accommodated in the inner wall of Eppendorf tubes, where 500 μl of microbial suspension was subsequently added. The microorganisms were then incubated under gentle shaking (150 r/min) in a rotary incubator (Tecnal-TE 4200) for 24 h at room temperature ($\pm 25^\circ\text{C}$) (Pagno et al., 2015).

As for the *P. expansum*, the stock culture grown in potato dextrose agar (PDA) (Kasvi) for seven days was suspended by adding sterilized Tween 80 solution (0.1% v/v) and scraped with a Drigalski loop to remove further spores to achieve a concentration of $0.72 \times 10^4\text{ log CFU/ml}$. It was then adjusted on a Neubauer (Kasvi) chamber using the saline solution (0.9%) (Avila-Sosa et al., 2010).

A 100 μl microbial suspension aliquot was then withdrawn from each tube and transferred to an Eppendorf containing 900 μl of 0.9% saline solution, followed by serial dilutions, while each of these solutions was vigorously vortexed. From each dilution, 10 μl of the microbial solution was seeded onto a tryptic soy agar

(Kasvi) or PDA medium (for *P. expansum*) and incubated at 37 °C for 24 h for Gram-negative bacteria. The incubation was performed at 37 °C for 48 h and 25 °C for 72 h for Gram-positive bacteria and *P. expansum*, respectively. Viable cells in each of the previously inoculated Petri dishes were counted to quantify the colony formation (Avila-Sosa et al., 2010; Pagno et al., 2015).

Shake-flask assay. The control and AgNP-containing films were shaped into eight 2 cm × 1.5 cm (3 cm²) rectangles and disinfected by immersing in 70% ethyl alcohol for 15 min before being dipped in 100 ml of TSB (Jokar et al., 2012).

Each bacterium (1 ml) was inoculated into 200 ml Erlenmeyer flasks containing TSB, test specimens, and 0.4 g of Tween 80 to achieve a final concentration of 1.13×10^5 log CFU/ml for *S. aureus*, 1.23×10^5 log CFU/ml for *E. faecalis*, 1.14×10^5 log CFU/ml for *E. coli*, and 1.10×10^5 for *S. Typhimurium* in log CFU/ml. After this process, the flasks were incubated under stirring at 150 r/min, 37 °C, and 26 h. Microbial growth was monitored with absorbance readings at 600 nm on a UV–VIS spectrometer using samples withdrawn every 2 h during 14 h; after this period, 24 and 26 h samples were also collected (Jokar et al., 2012).

Bacterial images from SEM. The SEM was conducted using a JSM-6701F/JEOL microscope to observe the antimicrobial activity of nanostructured films against Gram-positive *S. aureus* (1.08×10^7 log CFU/ml) and Gram-negative *E. coli* (1.36×10^6 log CFU/ml). The bacteria were initially added to the direct contact antimicrobial assay without serial dilutions. Ten microliters of the bacterial suspension was placed in the center spot of a microscopy slide previously coated with 0.1% poly-L-lysine solution. The slides were placed in Eppendorf flasks, which were then filled with Karnawesk solution for 4 h. Then, the samples were washed with cacodylate buffer and distilled water and dehydrated with 30% (10 min), 50% (10 min), 70% (10 min), 90% (10 min), and 100% (three times for 10 min each) acetone solutions. The samples were freeze-dried (Liotop L 101) according to the manufacturer's instructions for 24 h and retained in a desiccator until they were fixed onto stubs and gold-sputtered (Spricigo et al., 2015).

Statistical analysis

The analysis of variance (ANOVA) and Games–Howell multiple comparisons test were performed to evaluate the number of colonies concerning different AgNP concentrations in the direct contact antimicrobial assay, as

Bartlett's test indicated heterogeneity among variances. For the shake-flask antimicrobial assay, the variables were compared by ANOVA in addition to performing Duncan's multiple range test and Kruskal–Wallis test, respectively, for homogenous and heterogeneous samples on the variances resulting from Bartlett's test. All statistical procedures were conducted using the R software version 3.3.3 at a significance level of 5%. All microbiological evaluations were performed in triplicate.

RESULTS AND DISCUSSION

Film characterization

FEG-SEM. The images obtained from the backscattered FEG (Figure 1) exhibit light clusters. The gray portions of Ag and SiO₂ dispersed within the film on its surfaces and cross-sections, corroborating with the FEG images of the Ag + SiO₂ powder additive (Figure 2), thereby establishing the nanostructured form of the films.

The images obtained from the backscattered FEG include information on the deepest layers of the samples, which in turn depends on their atomic composition. In other words, because Ag and SiO₂ (which were present in the nanostructured LDPE films) possess a higher atomic number than the other film components, a better contrast is observed in these images (Figure 1) (Canevarolo, 2017), which corroborate the images of the surface of backscattered FEG Ag + SiO₂ powder additive.

The presence, on the surface and cross-sections of the films, of Ag and mesoporous silica such as AgNP carrier is of great importance, being that the first is a metal that demonstrates a wide range of bacterial fighting pathogens and is important for the potential antimicrobial properties of these films and the second is an inorganic substrate recognized for its biocompatibility, dispersibility, chemical stability, and ability to provide antimicrobial agents (Franci et al., 2015; Huang et al., 2015; Qasim et al., 2015).

FTIR. The infrared spectra presented in Figure 3 validate that the nanostructured samples demonstrate characteristic bands of pure LDPE. These results are similar to those observed in other studies that compared pure and AgNP-containing LDPE films (Becaro et al., 2015; Puti et al., 2014).

The bands at 719 cm⁻¹ (balance of methylene group sequences), 1369 cm⁻¹ (C–H flexion of methyl groups), 1461 cm⁻¹ (C–H folding of methylene groups), 2848 cm⁻¹ (C–H stretching), and 2916 cm⁻¹ (methylene stretching) corroborate the characteristic LDPE peaks (Mishra and Luyt, 2008; Olmos et al., 2012; Rajandas et al., 2012).

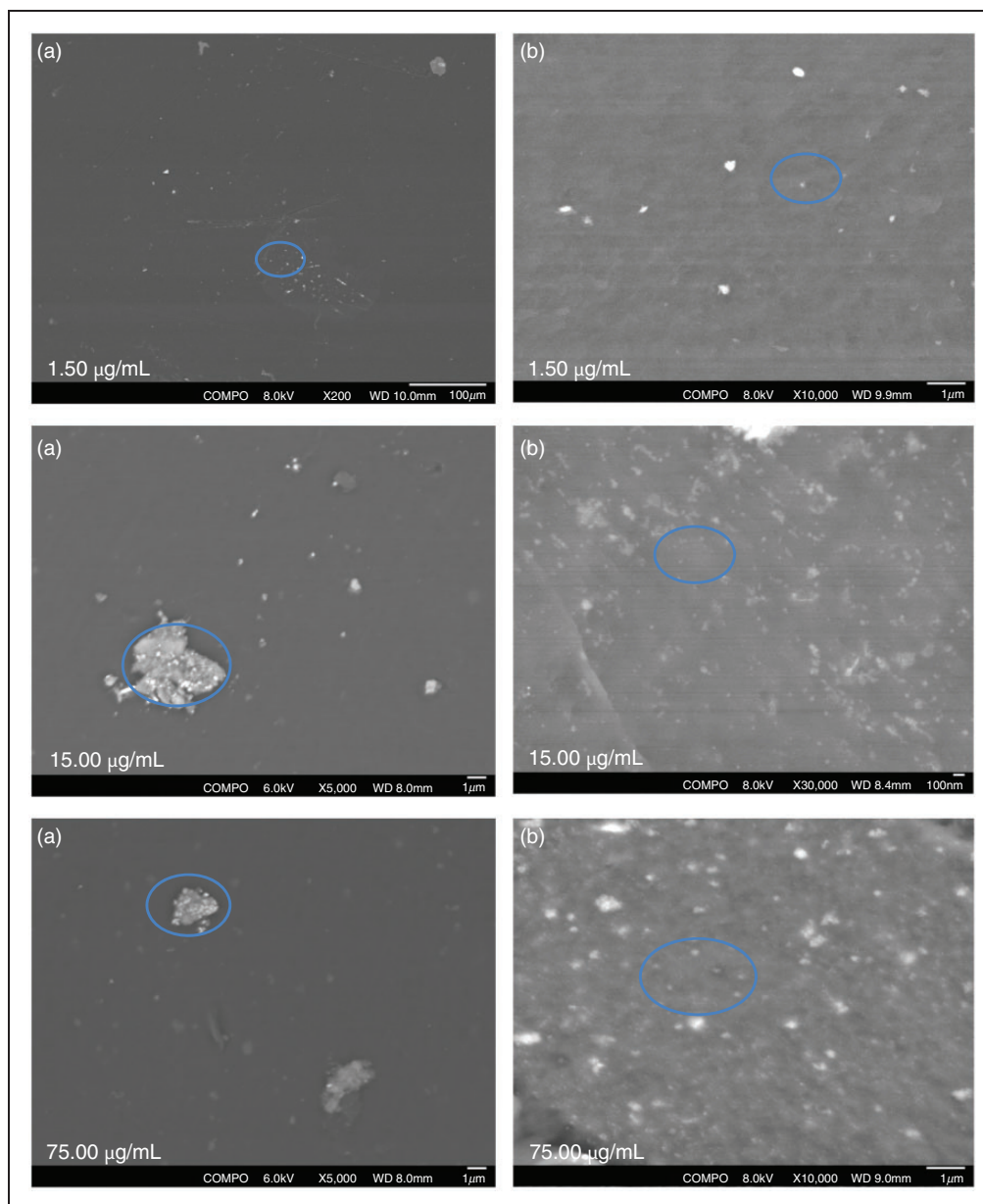


Figure 1. Surface (a) and cross-sectional (b) images, indicating the Ag and SiO₂ clusters obtained from backscattered FEG of nanostructured samples.

Figure 3 also shows peaks at 472 and 1087 cm^{-1} that are characteristic of SiO₂, which are assigned to tetragonal Si–O bonds and Si–O–Si group, respectively (Gowri et al., 2011; Lacerda Júnior et al., 2013). Also, it is observed that as the SiO₂ concentration increases, there is an increase in the corresponding peaks.

XRD. The XRD patterns of the films (Figure 4) show typical diffraction peaks around $2\theta = 21.56^\circ$, 24.08° , and 36.50° , which correspond to the orthorhombic structure of polyethylene. Such a pattern is similar to those reported in previous works on LDPE (Miranda

and Carvalho, 2011; Motaung et al., 2017; Xia et al., 2006).

The XRD patterns evidence two major crystalline peaks, the most intense in the angular range, which is the Miller index $[(110) - 22^\circ]$, and a less intense one $[(200) - 37^\circ]$, confirming the semi-crystallinity of polyethylene and characterize LDPE by matching with its specific crystallographic planes (Madani, 2011; Motaung et al., 2017).

There is an increase in the intensity of the peaks corresponding to the 3.75 and $7.50\text{ }\mu\text{g/ml}$ samples. This can be due to the mechanical stretching that may

have occurred during the processing of the films (LeBourvellec et al., 1986).

It is evident from Figure 4 that only the diffraction peaks of polyethylene are present in all the analyzed samples, indicating that the silica, AgNP carrier, is in its amorphous form, corroborating the absence of silica peaks in the Ag + SiO₂ powder additive. The lack of Ag in the outcome may be attributed to its low concentration in the samples, i.e. below the detection threshold of the equipment. Becaro et al. (2015) also studied AgNP-containing LDPE-based films using XRD and did not identify Ag.

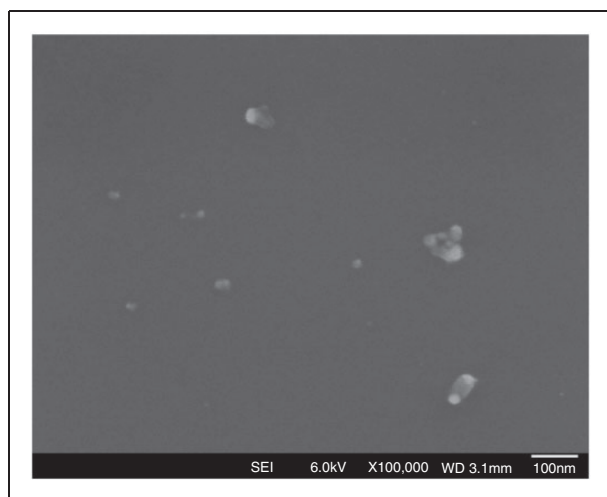


Figure 2. Surface images obtained from backscattered FEG of Ag + SiO₂ powder additive.

The diffraction peaks corresponding to Ag crystallographic planes are $2\theta = [(111) 38.2^\circ\text{--}39.4^\circ]$, $[(200) 44.4^\circ\text{--}44.6^\circ]$, $[(220) 63.5^\circ\text{--}64.6^\circ]$, and $[(311) 77.6^\circ\text{--}78.1^\circ]$ (Abdel-Mohsen et al., 2014; Liu et al., 2012).

Thermal analyses

TG. The nanostructured films exhibit thermal stabilities that are similar to those of the control film (Figure 5), which is better determined from the TG

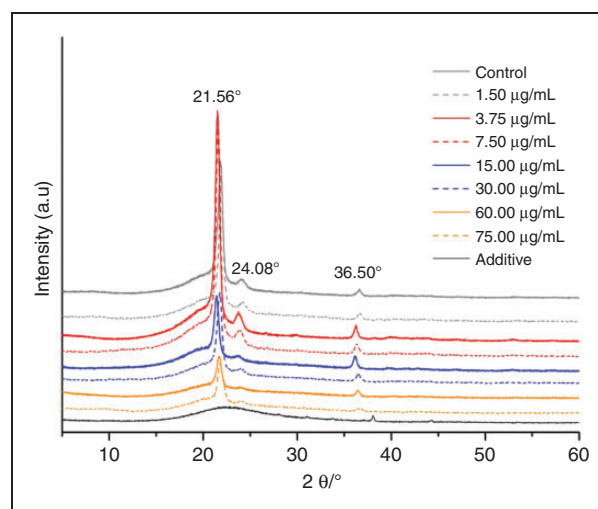


Figure 4. Intensity in arbitrary units (a.u.) versus diffraction angle in degrees ($2\theta^\circ$) for control and nanostructured samples and Ag + SiO₂ powder additive.

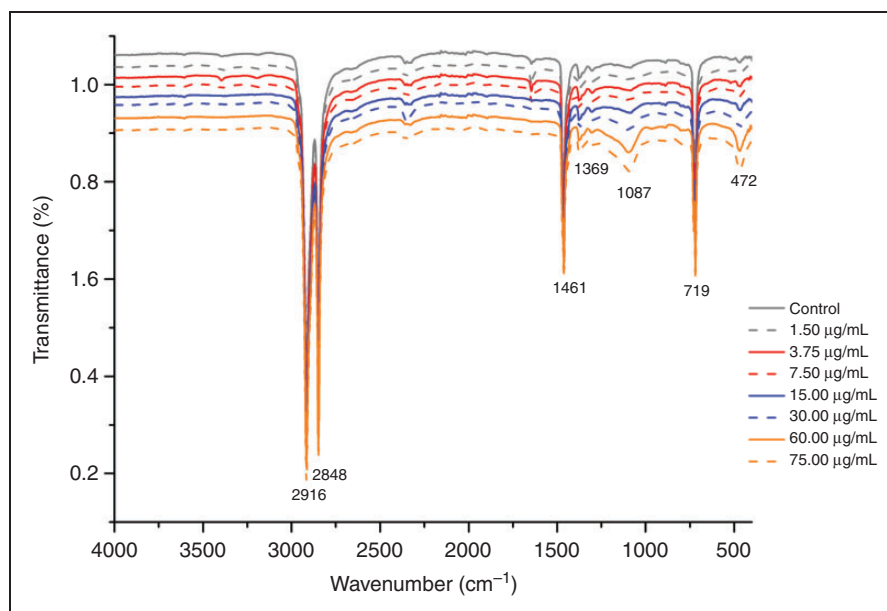


Figure 3. Transmittance (%) versus wavenumber (cm^{-1}) of control and nanostructured samples.

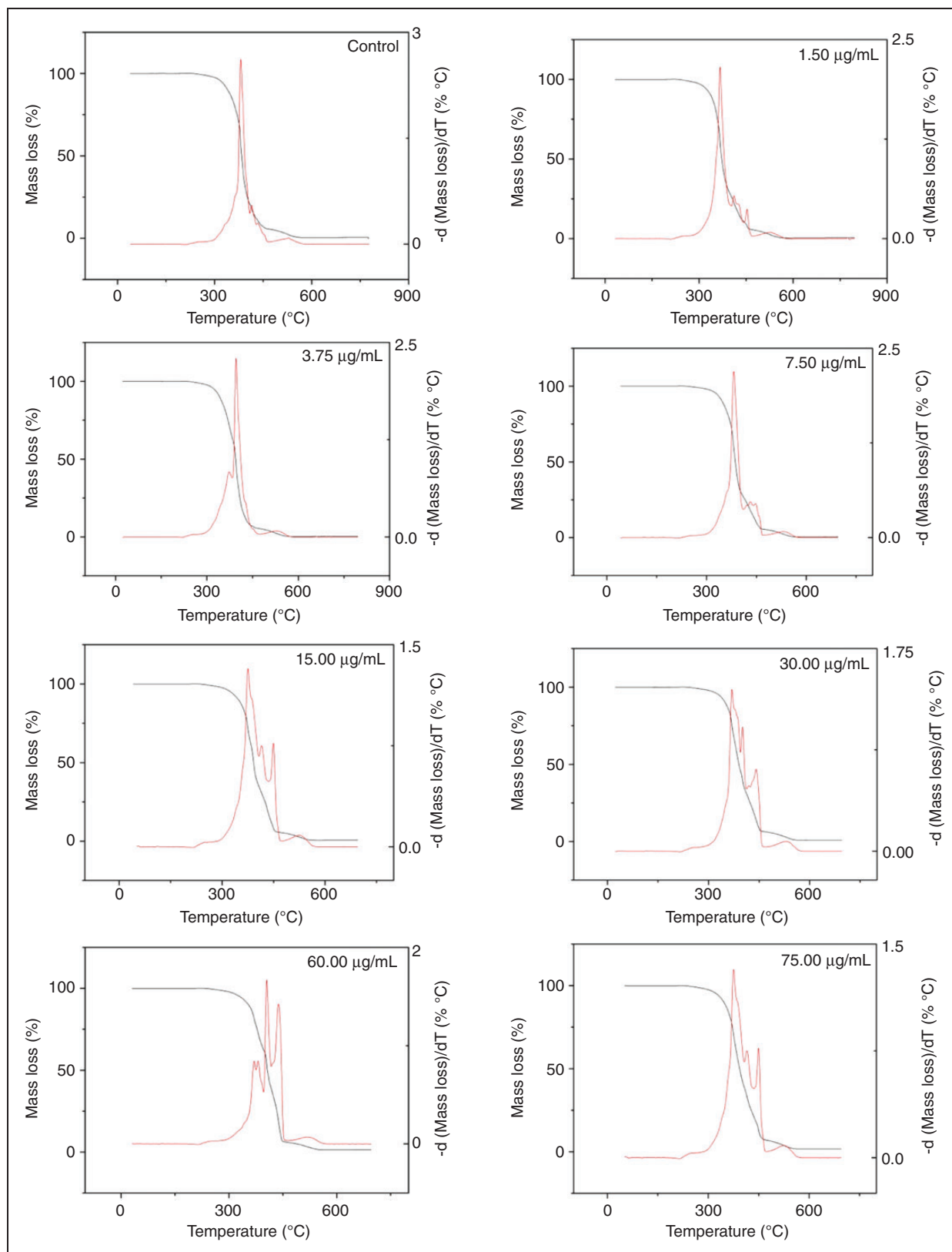


Figure 5. TG analysis and derivative thermogravimetric analysis curves of control and nanostructured samples in a synthetic air atmosphere at 10–800 °C.

curve than the derivative thermogravimetric analysis. This phenomenon is also evident from the extrapolated onset degradation temperatures (T_{onset}) of the films (Table 3). The T_{onset} has marginally declined in most samples when compared to control; however, it has marginally increased for concentrations of 3.75 and 60.00 $\mu\text{g/ml}$; this variation in the thermal stability of the samples may occur due to the distinct characteristics and syntheses between the masterbatch LDPE and the LDPE pellets used to process the films (Becaro et al., 2015). This observation corroborates the data reported by Boschetto et al. (2012), who observed that the addition of Ag-loaded zeolite into LDPE does not cause a significant difference in T_{onset} when compared to pristine LDPE.

The nanostructured samples exhibit a 50% degradation temperature residue ($T_{50\%}$) values similar to those of the control LDPE. Moreover, the residual percentage at 700 °C (Table 3) is similar to that of pristine LDPE (control), suggesting a suitable homogeneous polymer system (Becaro et al., 2015).

DSC. The melting temperature (T_m) of LDPE obtained from DSC was observed to be similar to the corresponding values reported in previous studies: 107.7, 114, and 124.5 °C (Boschetto et al., 2012; Motaung et al., 2017; Pérez et al., 2014). Moreover, it was observed that the addition of AgNPs did not promote significant T_m variations.

All the films analyzed exhibit endothermic peaks precisely related to the melting point of the polymer matrix, as the degradation temperature of the samples is observed only at higher temperatures (Figure 6). A similar outcome has been reported by Becaro et al. (2015), who compared the T_m values of pure and AgNP-added LDPE films and indicated no significant

variations in the melting temperature upon the addition of AgNPs (Boschetto et al., 2012).

Some variations are observed in the melting enthalpy (ΔH_m) corresponding to the nanostructured samples (Table 4). The decrease in ΔH_m corresponding to samples 30.00 and 60.00 $\mu\text{g/ml}$ and their increase of T_m when compared to the control film may be attributed to the strong interaction between masterbatch and polymer matrix to achieve a homogeneous distribution. This decreases the molecular mobility upon heating and thus decreases the energy absorbed during the process (Becaro et al., 2015).

Microbiological evaluations

Direct contact antimicrobial activity. The results obtained from this assay show that the nanostructured films exhibit antimicrobial activity against the tested

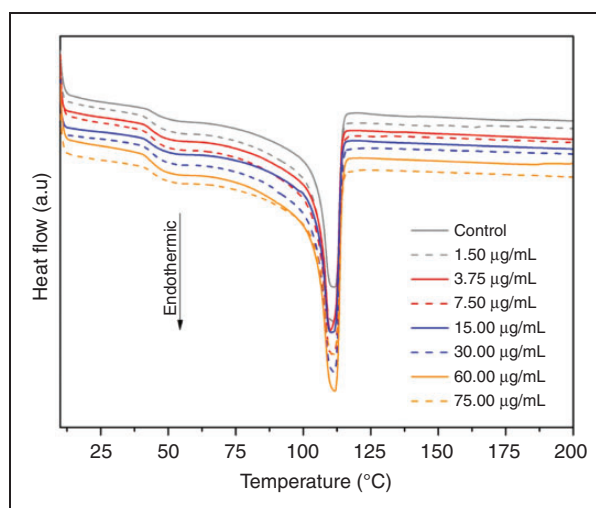


Figure 6. Heat flow (a.u.) versus temperature (°C) of control and nanostructured samples.

Table 3. Extrapolated onset degradation temperature (T_{onset}), the temperature was corresponding to 50% degradation ($T_{50\%}$) and residual percentage at 700 °C (R(%)) of control and nanostructured samples ($\mu\text{g/ml}$)

Concentrations ($\mu\text{g/ml}$)	T_{onset} (°C)	$T_{50\%}$ (°C)	R/700 °C (%)
Control	365.70	383.65	99.61
1.50	349.53	372.27	99.56
3.75	374.33	386.40	99.74
7.50	364.14	386.40	99.60
15.00	362.45	391.79	99.40
30.00	351.64	389.94	99.20
60.00	375.27	406.65	98.56
75.00	354.55	393.02	98.22

Table 4. Melting temperature (T_m) and enthalpy (ΔH_m) of control and nanostructured samples ($\mu\text{g/ml}$)

Concentrations ($\mu\text{g/ml}$)	T_m (°C)	ΔH_m (J/g)
Control	111.49	128.8
1.50	111.29	125.3
3.75	110.07	128.6
7.50	110.60	138.9
15.00	110.29	133.9
30.00	111.57	121.4
60.00	111.67	122.5
75.00	110.93	125.0

microorganisms (Table 5). It is observed that the log CFU/ml of *S. aureus*, *E. coli*, *S. Typhimurium*, and *P. expansum* decline for AgNP concentrations equal to or higher than 1.50 µg/ml, although the differences from the negative control were significant in most of these microorganisms ($p \leq 0.05$) only from the concentration of 3.75 µg/ml AgNPs.

Total inhibition of *P. expansum* growth was observed in all concentrations of AgNPs in the film. It is important to highlight that *P. expansum* is a significant concern of the global food industry due to its wide occurrence and ability to produce various mycotoxins, of which the most significant is patulin (Tannous et al., 2018).

In the case of *E. faecalis*, a reduced log CFU/ml at a concentration of 7.50 µg/ml is observed. However, a significant difference ($p \leq 0.05$) compared to the negative control is only observed at 75.00 µg/ml, suggesting that the highest concentration inhibits this microorganism.

Related to verified results, the antibacterial actions of silver nanoparticles may occur due to:

- Silver nanoparticles provide a large surface area for contact with microorganisms, thus enabling more significant contact between the particles and the cell membrane, facilitating their penetration into microorganisms (Durán et al., 2016; Zhang et al., 2016);
- Silver nanoparticles can impair DNA replication and, consequently, in the respiratory chain, resulting in cell death (Durán et al., 2016);
- Generation of reactive oxygen species (ROS) by silver nanoparticles, contributing to direct damage to a cell membrane (Durán et al., 2016; Zhang et al., 2016).

One of the main mechanisms of action of silver nanoparticles in microorganisms is their cell membrane dissolution, becoming important the species of microorganisms, since the antimicrobial activity of nanoparticles may depend on it (Durán et al., 2016; Zhang et al., 2016); in a research conducted by Kim et al. (2007) founded that the inhibitory effect of silver nanoparticles was more potent in yeast and *E. coli* than *S. aureus*; similar to the results in this research where the inhibitions of Gram-negative bacteria and *P. expansum* are significantly higher than those of Gram-positive bacteria, related to this we can suggest that the antimicrobial effect of AgNPs could be associated with the characteristics of specific bacterial species (Kim et al., 2007; Ruparelia et al., 2008). Gram-positive and Gram-negative bacteria present different membrane structures, particularly concerning the thickness of the peptidoglycan layer, which has an essential function in the protection of bacterium against antibacterial agents. Gram-positive bacteria feature a thicker peptidoglycan layer than their Gram-negative counterparts, and therefore, the former is more effectively protected against the formation of ruptures in their cell membranes, corroborating the inhibition values observed in this study and some prior studies as well (Kim et al., 2007, 2011; Mirzajani et al., 2011; Ruparelia et al., 2008).

Regarding DNA, silver ions at µmol/l levels impair replication due to the decoupling of respiratory electron transport from oxidative phosphorylation, which consequently inhibits respiratory chain enzymes and interferes with membrane permeability (Durán et al., 2016).

The accumulation of silver nanoparticles in the microbial membrane generates ROS that can seriously damage cellular components such as proteins, lipids, and nuclear substances, seriously destroying the

Table 5. Mean± and standard deviation values of *S. aureus*, *E. faecalis*, *E. coli*, *S. Typhimurium*, and *P. expansum* counts (log CFU/ml) of the negative control and nanostructured samples (µg/ml)

Concentrations (µg/ml)	<i>S. aureus</i> (log CFU/ml)	<i>E. faecalis</i> (log CFU/ml)	<i>E. coli</i> (log CFU/ml)	<i>S. Typhimurium</i> (log CFU/ml)	<i>P. expansum</i> (log CFU/ml)
Negative control	2.210 ± 1.834 ^a	1.196 ± 0.462 ^b	2.198 ± 1.322 ^a	1.809 ± 1.274 ^a	0.568 ± 0.079 ^a
1.50	2.035 ± 1.633 ^{ab}	1.493 ± 0.978 ^a	2.072 ± 0.623 ^b	1.625 ± 0.898 ^{ab}	<1
3.75	2.034 ± 1.635 ^{ab}	1.225 ± 0.845 ^{bc}	1.880 ± 1.243 ^c	1.535 ± 0.477 ^b	<1
7.50	1.828 ± 1.134 ^b	1.188 ± 0.740 ^{bc}	1.852 ± 1.253 ^c	1.276 ± 0.875 ^c	<1
15.00	1.818 ± 0.556 ^b	1.179 ± 0.568 ^b	1.588 ± 0.914 ^d	0.672 ± 0.079 ^d	<1
30.00	1.817 ± 1.068 ^b	1.104 ± 0.531 ^{bc}	0.845 ± 0.519 ^e	0.771 ± 0.079 ^d	<1
60.00	1.780 ± 1.322 ^{bc}	0.996 ± 0.857 ^{bc}	0.672 ± 0.144 ^e	0.699 ± 0.505 ^d	<1
75.00	1.682 ± 0.398 ^c	0.934 ± 0.380 ^c	0.279 ± 0.041 ^f	<1	<1

Mean values followed by the same letter (a, b, c, d, e or f) within the same column do not differ significantly, as indicated by Duncan and Kruskal–Wallis (*S. Typhimurium*) tests ($p > 0.05$).

Table 6. Mean± and standard deviation values of growth rate, maximum concentrations at stationary and lag phases (reported in hours) of *S. aureus*, *E. faecalis*, *E. coli*, and *S. Typhimurium* of negative control and nanostructured samples (µg/ml)

Microorganism/ Concentration (µg/ml)	Growth rate (abs.)	Stationary phase (abs.)	Lag phase (h)
<i>S. aureus</i>			
Negative control	0.31 ± 0.01 ^a	2.51 ± 0.06 ^a	5:59:20 ± 0:03:03 ^{cd}
1.50	0.30 ± 0.01 ^a	2.51 ± 0.04 ^a	5:56:20 ± 0:15:32 ^d
3.75	0.31 ± 0.01 ^a	2.51 ± 0.03 ^a	6:14:40 ± 0:10:01 ^{bbc}
7.50	0.32 ± 0.00 ^a	2.48 ± 0.03 ^a	6:18:20 ± 0:08:23 ^{bbc}
15.00	0.31 ± 0.01 ^a	2.51 ± 0.02 ^a	6:26:00 ± 0:08:40 ^{bc}
30.00	0.31 ± 0.01 ^a	2.49 ± 0.05 ^a	6:34:40 ± 0:03:13 ^b
60.00	0.30 ± 0.02 ^a	2.50 ± 0.05 ^a	6:34:40 ± 0:19:01 ^b
75.00	0.31 ± 0.02 ^a	2.48 ± 0.02 ^a	6:39:40 ± 0:28:27 ^b
Positive control	0.01 ± 0.00 ^b	0.10 ± 0.00 ^b	8:43:40 ± 0:22:11 ^a
<i>E. faecalis</i>			
Negative control	0.57 ± 0.04 ^a	1.57 ± 0.02 ^a	5:51:40 ± 0:03:13 ^a
1.50	0.53 ± 0.06 ^a	1.56 ± 0.01 ^a	5:53:00 ± 0:05:34 ^a
3.75	0.54 ± 0.02 ^a	1.55 ± 0.01 ^{abc}	5:57:00 ± 0:02:00 ^a
7.50	0.53 ± 0.02 ^a	1.53 ± 0.01 ^{bc}	5:56:00 ± 0:02:00 ^a
15.00	0.52 ± 0.03 ^{ab}	1.52 ± 0.02 ^{bc}	5:58:20 ± 0:04:02 ^a
30.00	0.51 ± 0.06 ^{ab}	1.52 ± 0.01 ^c	5:58:20 ± 0:01:09 ^a
60.00	0.44 ± 0.05 ^{bc}	1.52 ± 0.03 ^{bc}	5:56:00 ± 0:06:15 ^a
75.00	0.38 ± 0.04 ^c	1.52 ± 0.01 ^c	5:57:40 ± 0:10:58 ^a
Positive control	-0.01 ± 0.01 ^d	0.30 ± 0.01 ^d	1:21:40 ± 2:21:27 ^b
<i>E. coli</i>			
Negative control	0.32 ± 0.03 ^{ab}	2.09 ± 0.02 ^a	5:34:40 ± 0:14:22 ^b
1.50	0.37 ± 0.04 ^a	2.01 ± 0.01 ^{bc}	6:00:20 ± 0:17:09 ^b
3.75	0.36 ± 0.09 ^a	2.02 ± 0.05 ^{abc}	5:57:20 ± 0:32:08 ^b
7.50	0.32 ± 0.03 ^a	2.02 ± 0.05 ^{abc}	5:49:00 ± 0:18:15 ^b
15.00	0.35 ± 0.10 ^a	2.01 ± 0.05 ^{bc}	5:54:40 ± 0:43:25 ^b
30.00	0.54 ± 0.38 ^a	1.98 ± 0.05 ^{bc}	6:42:40 ± 1:32:05 ^b
60.00	0.45 ± 0.16 ^a	1.96 ± 0.06 ^c	6:46:20 ± 0:47:00 ^b
75.00	0.34 ± 0.03 ^a	2.06 ± 0.05 ^{ab}	7:03:40 ± 0:49:54 ^b
Positive control	0.04 ± 0.04 ^b	0.09 ± 0.00 ^d	10:26:00 ± 0:54:35 ^a
<i>S. Typhimurium</i>			
Negative control	0.19 ± 0.00 ^a	2.50 ± 0.00 ^a	2:47:00 ± 0:06:56 ^b
1.50	0.20 ± 0.00 ^a	2.48 ± 0.01 ^{ab}	2:52:20 ± 0:14:11 ^b
3.75	0.19 ± 0.00 ^a	2.48 ± 0.01 ^b	2:51:20 ± 0:03:03 ^b
7.50	0.19 ± 0.00 ^a	2.47 ± 0.01 ^b	2:58:00 ± 0:13:45 ^b
15.00	0.20 ± 0.00 ^a	2.36 ± 0.02 ^c	3:02:40 ± 0:06:30 ^b
30.00	0.20 ± 0.00 ^a	2.33 ± 0.10 ^c	3:05:20 ± 0:11:35 ^b
60.00	0.19 ± 0.00 ^a	2.32 ± 0.06 ^c	2:55:40 ± 0:09:37 ^b
75.00	0.20 ± 0.01 ^a	2.25 ± 0.08 ^c	3:27:20 ± 0:14:34 ^b
Positive control	0.15 ± 0.02 ^b	2.00 ± 0.00 ^d	11:42:20 ± 2:27:33 ^a

Mean values followed by the same letter (a, b, c or d) within the same column do not differ significantly, as indicated by Duncan and Kruskal-Wallis (*S. Typhimurium*) tests ($p > 0.05$).

integrity of cell membranes, inducing or increasing cell permeability, causing death (Durán et al., 2016; Zhang et al., 2016).

The low inhibition observed concerning *E. faecalis* may be related to its membrane structure and ability to form biofilms, which renders it more resistant to phagocytosis, antibodies, and antimicrobial agents (Alabdulmohsen and Saad, 2017). In contrast, Wu et al. (2014) pointed out that the excellent performance of AgNPs against *E. faecalis* depends not only on the concentration of both species but also on the interaction time.

Furthermore, it was verified that the higher the AgNPs' concentration in the sample, the greater the inhibition, suggesting an improved antimicrobial effect of AgNP-added LDPE films. This outcome is similar to that observed by Ruparelia et al. (2008), who studied the biocidal effect of AgNPs against *E. coli* and *S. aureus*.

Shake-flask assay. The results obtained from the shake-flask assays show that the nanostructured films influence the growth kinetics of *S. aureus*, *E. faecalis*, *E. coli*, and *S. Typhimurium*. These results are presented in Table 6.

Regarding the growth rate, only *E. faecalis* demonstrates a significant difference from the negative control ($p \leq 0.05$) at 60.00 $\mu\text{g/ml}$, suggesting that AgNPs' addition to the films supports the reduction in the growth rate of such bacterium.

As for the maximum concentration at the stationary phase, it is observed that the nanostructured samples lead to decreased bacterial counts, although only *E. faecalis*, *E. coli*, and *S. Typhimurium* appear

significantly different ($p \leq 0.05$) from the negative control at concentrations 7.50, 1.50, and 3.75 $\mu\text{g/ml}$, respectively. These results indicate that the lowest concentrations are more effective in reducing the counts of Gram-negative bacteria (*E. coli* and *S. Typhimurium*). Jokar et al. (2012) reported a similar outcome, according to which AgNPs reduced *S. aureus* and *E. coli* counts by 23.3 and 27.3%, respectively.

The lag phase is observed to last longer upon AgNPs' addition to LDPE-based films, corroborating the previously published results (Jokar et al., 2012; Kim et al., 2011; Sadeghnejad et al., 2014). *S. aureus*, notably, demonstrates a significant difference ($p \leq 0.05$) from the negative control at 30.00 $\mu\text{g/ml}$ and higher, suggesting that an average concentration may provide a more prolonged lag phase for the growth of *S. aureus*.

It is clear from the aforementioned analyses that nanostructured films inhibited the growth and reproduction of bacterial cells in the early stages. This observation is in line with the results of Sadeghnejad et al. (2014), who investigated the antimicrobial action of AgNP-added polyethylene films against *S. aureus* and *E. coli* using the shake-flask assays. They discovered that AgNPs influence the lag and log phases of both bacteria. Additionally, it was evidenced that the higher the AgNPs concentration ($\mu\text{g/ml}$) in LDPE-based films, the greater its influence on the growth kinetics of the studied bacteria. A similar outcome was observed by Jokar et al. (2012), who studied the effect of AgNPs on LDPE films using shake-flask assays. They also noticed that nanocomposites comprising low AgNPs contents did not alter the growth kinetics of *S. aureus* and *E. coli*.

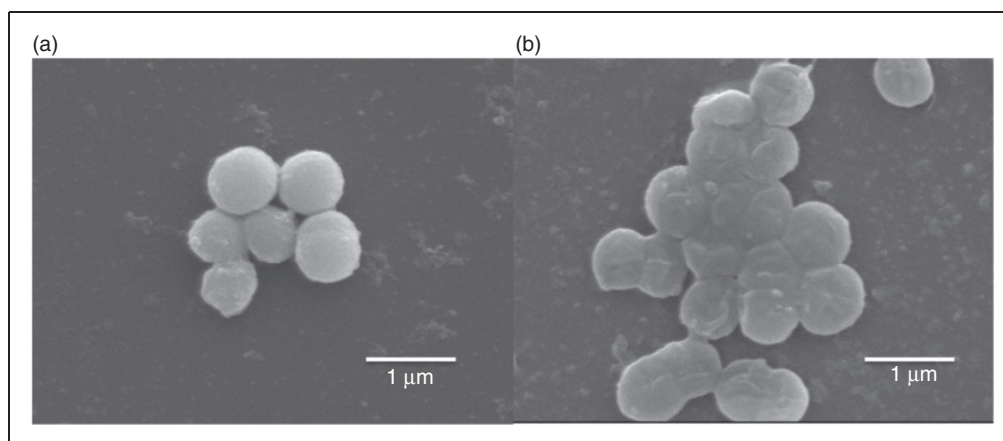


Figure 7. *S. aureus* treated with control (a) and nanostructured (75.00 $\mu\text{g/ml}$) (b) LDPE-based films.

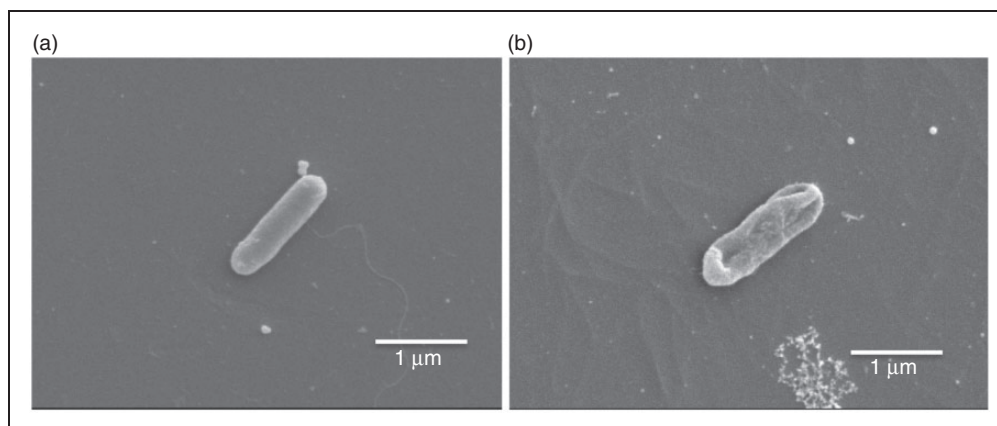


Figure 8. *E. coli* treated with control (a) and nanostructured (75.00 µg/ml) (b) LDPE-based films.

Bacterial images from SEM. *S. aureus* and *E. coli* were imaged after being in contact with the control and nanostructured films (75.00 µg/ml); these images are shown in Figures 7 and 8, respectively. Both present bacteria alteration of the microbial wall structure upon treatment with AgNP-enriched LDPE films.

The mechanism of action of AgNPs as an antimicrobial agent has not been completely elucidated yet, although some models have already been proposed (Prabhu and Poulose, 2012). Sondi and Salopek-Sondi (2004) verified using SEM that the surface of the bacterial cell wall upon contact with the AgNPs conceivably promotes structural changes in the wall structure (e.g. increase permeability), thereby impairing the ability of the bacterial cells in suitably regulating the transport across the plasma membrane and ultimately causing cell death.

The critical changes to the membrane structure observed in AgNP-treated bacteria (Figures 7(b) and 8(b)) may be a consequence of the ability of silver nanoparticles to anchor in the cell wall and accumulate to form “pits” on the cell surface. Silver nanoparticles, after contact with the cell membrane surface, suffer a change in their respiration, because silver interacts with the enzymes of the microorganisms, which can cause a degradation of the membrane structure (Prabhu and Poulose, 2012; Raffi et al., 2008).

CONCLUSION

It is established from this study that the addition of AgNPs into LDPE films interfered neither in the physicochemical nor thermal properties of the latter. LDPE/AgNPs films were effective in inhibiting the growth of the investigated microorganisms. AgNPs exhibited a more significant antimicrobial action against Gram-negative bacteria and fungi than Gram-positive bacteria. These results demonstrated the

potential of extruding LDPE films after being incorporated with AgNPs for producing antimicrobial food packaging, especially for liquid foods. It was verified through microbiological evaluations using direct contact antimicrobial activity and shake-flask assays that such films can lead to diminishing contamination risks and maintaining food quality.

ACKNOWLEDGEMENTS

The authors are grateful to Universidade Estadual Paulista “Júlio de Mesquita Filho” (UNESP), and Empresa Brasileira de Pesquisa Agropecuária (EMBRAPA, project 13.16.04.041.00.00) for financial and technical support.


DECLARATION OF CONFLICTING INTERESTS

The author(s) declared no potential conflicts of interest with respect to the research, authorship, and/or publication of this article.

FUNDING

The author(s) received no financial support for the research, authorship, and/or publication of this article: The author(s) received financial support for this research from Coordenação de Aperfeiçoamento de Pessoal de Nível Superior-Brasil (CAPES)—Finance Code 1633026, Conselho Nacional de Desenvolvimento Científico e Tecnológico (CNPq), Fundação de Amparo à Pesquisa do Estado de São Paulo (FAPESP) and Empresa Brasileira de Pesquisa Agropecuária (EMBRAPA, project 13.16.04.041.00.00).

ORCID iDs

Sabrina da Costa Brito  <https://orcid.org/0000-0002-0868-254X>

Marcos D Ferreira  <https://orcid.org/0000-0003-4544-8784>

REFERENCES

Abdel-Mohsen AM, Abdel-Rahman RM, Fouda MMG, Vojtova L, Uhrova L, Hassan AF, et al. (2014).

- Preparation, characterization and cytotoxicity of schizophyllan/silver nanoparticle composite. *Carbohydrate Polymers* 102: 238–245.
- Akter M, Sikder MT, Rahman MM, Ullah AKMA, Hossain KFB, Banik S, et al. (2018). A systematic review on silver nanoparticles-induced cytotoxicity: Physicochemical properties and perspectives. *Journal of Advanced Research* 9: 1–16.
- Alabdulmohsen ZA and Saad AY. (2017). Antibacterial effect of silver nanoparticles against *Enterococcus faecalis*. *Saudi Endodontic Journal* 7(1): 29.
- Avila-Sosa R, Hernández-Zamoran E, López-Mendoza I, Palou E, Munguía MTJ, Nevárez-Moorillón GV and López-Malo A. (2010). Fungal inactivation by mexican oregano (*lippia berlandieri schauer*) essential oil added to amaranth, chitosan, or starch edible films. *Journal of Food Science* 75(3): 127–133.
- Becaro AA, Puti FC, Correa DS, Paris EC, Marconcini JM and Ferreira MD. (2015). Polyethylene films containing silver nanoparticles for applications in food packaging: Characterization of physico-chemical and anti-microbial properties. *Journal of Nanoscience and Nanotechnology* 15(3): 2148–2156.
- Becaro AA, Puti FC, Panosso AR, Gern JC, Brandão HM, Correa DS, et al. (2016). Postharvest quality of fresh-cut carrots packaged in plastic films containing silver nanoparticles. *Food and Bioprocess Technology* 9(4): 637–649.
- Boschetto DL, Lerin L, Cansian R, Pergher SBC and Di Luccio M. (2012). Preparation and antimicrobial activity of polyethylene composite films with silver exchanged zeolite-Y. *Chemical Engineering Journal* 204–205: 210–216.
- Brody AL, Bugusu B, Han JH, Sand CK and McHugh TH. (2008). Innovative food packaging solutions. *Journal of Food Science* 73(8): 107–116.
- Canevarolo SV. (2017). Microscopia Eletrônica da Varredura. In: SV Canevarolo (ed.), *Técnicas de Caracterização de Polímeros*, 3rd edn, Artliber, São Paulo, p. 448.
- Carbone M, Donia DT, Sabbatella G and Antiochia R. (2016). Silver nanoparticles in polymeric matrices for fresh food packaging. *Journal of King Saud University – Science* 28(4): 273–279.
- Chaudhry Q, Scotter M, Blackburn J, Ross B, Boxall A, Castle L, et al. (2008). Applications and implications of nanotechnologies for the food sector. *Food Additives and Contaminants – Part A Chemistry, Analysis, Control, Exposure and Risk Assessment* 25(3): 241–258.
- Chen X and Schluesener HJ. (2008). Nanosilver: A nanoprodukt in medical application. *Toxicology Letters* 176(1): 1–12.
- Damm C, Neumann M and Münstedt H. (2005). Properties of nanosilver coatings on polymethyl methacrylate. *Soft Materials* 3(2–3): 71–88.
- Dehnavi A, Aroujalian A, Raisi A and Fazel S. (2012). Preparation and characterization of polyethylene/silver nanocomposite films with antibacterial activity. *Journal of Applied Polymer Science* 127(2): 1180–1190.
- Del Nobile MA, Conte A, Buonocore GG, Incoronato AL, Massaro A and Panza O. (2009). Active packaging by extrusion processing of recyclable and biodegradable polymers. *Journal of Food Engineering* 93(1): 1–6.
- Duncan TV. (2011). Applications of nanotechnology in food packaging and food safety: Barrier materials, antimicrobials and sensors. *Journal of Colloid and Interface Science* 363(1): 1–24.
- Durán N, Durán M, de Jesus MB, Seabra AB, Fávaro WJ and Nakazato G. (2016). Silver nanoparticles: A new view on mechanistic aspects on antimicrobial activity. *Nanomedicine: Nanotechnology, Biology, and Medicine* 12(3): 789–799.
- Emamifar A, Kadivar M, Shahedi M and Solimanian-Zad S. (2011). Effect of nanocomposite packaging containing Ag and ZnO on reducing pasteurization temperature of orange juice. *Journal of Food Processing and Preservation* 36(2): 104–112.
- Franci G, Falanga A, Galdiero S, Palomba L, Rai M, Morelli G, et al. (2015). Silver nanoparticles as potential antibacterial agents. *Molecules* 20(5): 8856–8874.
- Gava AJ, Silva CAB and Frias JRG. (2008). Embalagem de Alimentos. In: AJ Gava (ed.) *Tecnologia de Alimentos: Princípios e Aplicações*. 2nd edn, Nobel, São Paulo, pp. 105–127.
- Gowri LAVS, Amorim T, Carneiro N, Souto AP and Esteves MF. (2011). Novel copolymer for SiO₂ nanoparticles dispersion. *Journal of Applied Polymer Science* 124: 1553–1561.
- Greiner R. (2009). Current and projected applications of nanotechnology in the food sector. *Nutrire: Journal of the Brazilian Society for Food and Nutrition* 34(1): 243–260.
- Huang R, Hou B, Li H, Fu X and Xie C. (2015). RSC advances preparation of silver nanoparticles supported mesoporous silica microspheres with perpendicularly aligned mesopore channels and their antibacterial activities. *RSC Advances* 5: 61184–61190.
- Jokar M, Abdul Rahman R, Ibrahim NA, Abdullah LC and Tan CP. (2012). Melt production and antimicrobial efficiency of low-density polyethylene (LDPE)-silver nanocomposite film. *Food and Bioprocess Technology* 5(2): 719–728.
- Kim JS, Kuk E, Yu KN, Kim JH, Park SJ, Lee HJ, et al. (2007). Antimicrobial effects of silver nanoparticles. *Nanomedicine: Nanotechnology, Biology, and Medicine* 3(1): 95–101.
- Kim S, Lee H and Ryu D. (2011). Antibacterial activity of silver-nanoparticles against *Staphylococcus aureus* and *Escherichia coli*. *Korean Journal of Microbiology* 39(1): 77–85.
- Lacerda Júnior O. da S, Cavalcanti RM, Matos TM, Venâncio J. de B, Barros IB, Veiga-Júnior VF, et al. (2013). Síntese do material mesoporoso mcm-41 usando esponja de água-doce como fonte de sílica. *Química Nova* 36(9): 1348–1353.
- LeBourvellec G, Monnerie L and Jarry JP. (1986). Amorphous orientation and induced crystallization in uniaxially stretched poly(ethylene terephthalate glycol). *Polymer* 27(6): 856–860.
- Liu F, Liu H, Li X, Zhao H, Zhu D, Zheng Y, et al. (2012). Nano-TiO₂@Ag/PVC film with enhanced antibacterial

- activities and photocatalytic properties. *Applied Surface Science* 258(10): 4667–4671.
- Madani M. (2011). Structure, optical and thermal decomposition characters of LDPE graft copolymers synthesized by gamma irradiation. *Current Applied Physics* 11(1): 70–76.
- Marsh K and Bugusu B. (2007). Food packaging – Roles, materials, and environmental issues: Scientific status summary. *Journal of Food Science* 72(3): 39–55.
- Mihindukulasuriya S and Lim L. (2014). Nanotechnology development in food packaging: A review. *Trends in Food Science & Technology* 40(2): 149–167.
- Miranda VR and Carvalho AJF. (2011). Blendas compatíveis de amido termoplástico e polietileno de baixa densidade compatibilizadas com ácido cítrico. *Polímeros* 21(5): 353–360.
- Mirzajani F, Ghassempour A, Aliahmadi A and Esmaeili MA. (2011). Antibacterial effect of silver nanoparticles on *Staphylococcus aureus*. *Research in Microbiology* 162(5): 542–549.
- Mishra AK and Luyt AS. (2008). Effect of sol-gel derived nano-silica and organic peroxide on the thermal and mechanical properties of low-density polyethylene/wood flour composites. *Polymer Degradation and Stability* 93(1): 1–8.
- Motaung T, Mochane M, Makhetha T, Motloung S, Mokhothu T, Mokhena T, et al. (2017). Effect of mechanical treatment on morphology and thermal and mechanical properties of sugar cane bagasse-low-density polyethylene composites. *Polymer Composites* 38(8): 1497–1503.
- Olmos D, Martínez-Tarifa JM, González-Gaitano G and González-Benito J. (2012). Uniformly dispersed submicrometre BaTiO₃ particles in PS based composites. Morphology, structure and dielectric properties. *Polymer Testing* 31(8): 1121–1130.
- Pagno CH, Costa TMH, De Menezes EW, Benvenuti EV, Hertz PF, Matte CR, et al. (2015). Development of active biofilms of quinoa (*Chenopodium quinoa* W.) starch containing gold nanoparticles and evaluation of antimicrobial activity. *Food Chemistry* 173: 755–762.
- Pérez MA, Rivas BL, Garrido-Miranda KA, Campos-Requena VH, Martínez M, Castaño J, et al. (2014). Low density polyethylene (LDPE) nanocomposites with passive and active barrier properties. *Journal of the Chilean Chemical Society* 59(2): 2442–2446.
- Piringer OG and Baner AL. (2000). Preservation of quality through packaging. In: Piringer OG and Baner AL (eds) *Plastic Packaging Materials for Food: Barrier Function, Mass Transport, Quality Assurance, and Legislation*. 1st ed. Weinheim: Wiley-VCH, pp. 4–8.
- Prabhu S and Poulouse EK. (2012). Silver nanoparticles: Mechanism of antimicrobial action, synthesis, medical applications, and toxicity effects. *International Nano Letters* 2(1): 32.
- Puti FC, Becaro AA, Correa DS and Ferreira MD. (2014). Caracterização físico-química e microbiológica de filmes de PEBD com nanopartículas para aplicação como embalagens para alimentos. In: CMP Vaz, DMBP Milori and S. Crestana (eds) *Anais do SIAGRO: Ciência, Inovação e Mercado* 2014, vol. 1, Embrapa Instrumentação, São Carlos/SP, pp. 391–394.
- Qasim M, Singh BR, Naqvi AH, Paik P and Das D. (2015). Silver nanoparticles embedded mesoporous SiO₂ nanosphere: An effective anticandidal agent against *Candida albicans* 077. *Nanotechnology* 26(28): 285102.
- Raffi M, Hussain F, Bhatti TM, Akhter JI, Hameed A and Hasan MM. (2008). Antibacterial characterization of silver nanoparticles against *E. coli* ATCC-15224. *Journal of Materials Science and Technology* 24(2): 192–196.
- Rajandas H, Parimannan S, Sathasivam K, Ravichandran M and Su Yin L. (2012). A novel FTIR-ATR spectroscopy based technique for the estimation of low-density polyethylene biodegradation. *Polymer Testing* 31(8): 1094–1099.
- Ruparelia JP, Chatterjee AK, Duttagupta SP and Mukherji S. (2008). Strain specificity in antimicrobial activity of silver and copper nanoparticles. *Acta Biomaterialia* 4(3): 707–716.
- Sadeghnejad A, Aroujalian A, Raisi A and Fazel S. (2014). Antibacterial nano silver coating on the surface of polyethylene films using corona discharge. *Surface and Coatings Technology* 245: 1–8.
- Siddiqi KS, Husen A and Rao RAK. (2018). A review on biosynthesis of silver nanoparticles and their biocidal properties. *Journal of Nanobiotechnology* 16(1).
- Sondi I and Salopek-Sondi B. (2004). Silver nanoparticles as antimicrobial agent: A case study on *E. coli* as a model for Gram-negative bacteria. *Journal of Colloid and Interface Science* 275(1): 177–182.
- Spricigo PC, Trento JP and Bresolin JD. (2015). Methods of preparing flower stem samples for scanning electron microscopy. *Advances in Ornamental Horticulture and Landscaping* 21(1): 17–26.
- Tannous J, Keller NP, Atoui A, El Khoury A, Lteif R, Oswald IP, et al. (2018). Secondary metabolism in *Penicillium expansum*: Emphasis on recent advances in patulin research. *Critical Reviews in Food Science and Nutrition* 58(12): 2082–2098.
- Wróblewska-Krepsztul J, Rydzkowski T, Borowski G, Szczypiński M, Klepka T and Thakur VK. (2018). Recent progress in biodegradable polymers and nanocomposite-based packaging materials for sustainable environment. *International Journal of Polymer Analysis and Characterization* 23(4): 383–395.
- Wu D, Fan W, Kishen A, Gutmann JL and Fan B. (2014). Evaluation of the antibacterial efficacy of silver nanoparticles against *Enterococcus faecalis* biofilm. *Journal of Endodontics* 40(2): 285–290.
- Xia X, Cai S and Xie C. (2006). Water absorption characteristics of novel Cu/LDPE nanocomposite for use in intrauterine devices. *Journal of Biomedical Materials Research. Part B, Applied Biomaterials* 79(2): 345–352.
- Youssef AM and El-Sayed SM. (2018). Bionanocomposites materials for food packaging applications: Concepts and future outlook. *Carbohydrate Polymers* 193: 19–27.
- Zhang C, Hu Z and Deng B. (2016). Silver nanoparticles in aquatic environments: Physiochemical behavior and antimicrobial mechanisms. *Water Research* 88: 403–427.